Journal of South American Earth Sciences 96 (2019) 102349

Contents lists available at ScienceDirect

Journal of South American Earth Sciences

journal homepage: www.elsevier.com/locate/jsames

Sources of organic matter in two contrasting tropical coastal environments: The Caribbean Sea and the eastern Pacific

C. Huguet[a,*], J.-H. Kim[b,**], C. González-Arango[c], V. Ramírez-Valencia[c], S. Kang[d], J.-K. Gal[d], K.-H. Shin[d]

[a] Department of Geosciences, Universidad de Los Andes, Colombia
[b] Korea Polar Research Institute (KOPRI), 26 Songdomirae-ro, Yeonsu-gu, Incheon, 21990, South Korea
[c] Department of Biological Sciences, Universidad de los Andes, Bogotá, Colombia
[d] Hanyang University, 55 Hanyangdaehak-ro, Sangnok-gu, Ansan, 15588, South Korea

ARTICLE INFO

Keywords:
Glycerol dialkyl glycerol tetraethers (GDGTs)
n-alkanes
Terrestrial input
Caribbean
Eastern tropical pacific

ABSTRACT

In this study, we evaluate sources of organic matter (OM) in two contrasting tropical coastal environments in Colombia, using a combination of glycerol dialkyl glycerol tetraethers (GDGTs) and *n*-alkane lipid biomarkers. A clear difference between the less productive Caribbean Sea and the more productive eastern Pacific is observed, with higher terrestrial contributions into the eastern Pacific strongly associated with riverine inputs. Although higher land plant-derived *n*-alkanes can be transported as eolian dust, our results suggest mainly riverine sources for our samples. When looking at the branched GDGT compositions, in situ production could be identified in most Caribbean stations and some of the more coastal sites in the Pacific with $\#rings_{tetra}$ index values of above 0.7. The remaining stations in the eastern Pacific display soil-eroded GDGTs inputs associated with river discharges and deposited in the proximity of the coast. Marine production as measured by short chain *n*-alkanes and crenarchaeol are also higher in the eastern Pacific. It appears that the terrestrial inputs would bring nutrients as well as OM fueling both auto- and heterotrophs making the eastern Pacific overall more productive. We also observe OM of petrogenic origin, albeit in a low amount, especially in coastal Caribbean sites located near main harbors. This study helps improve the understanding of the complex mixture of OM inputs, origins and transport mechanisms into Colombian coastal areas. The present work emphasizes the need to integrate climate, geological setting and hydrology to fully understand the carbon cycle at a regional scale.

1. Introduction

Knowing the fate of terrestrial organic matter in the Oceans is crucial to understanding the global carbon cycle (e.g., Schlesinger and Melack, 1981; Zonneveld et al., 2010). The carbon cycle is one of the main drivers of earth's climate, and in view of the current climate change it is pressing to constrain not only the sinks but also the sources and transport pathways. Terrestrial carbon input to ocean is a long-term sink, and as such, transport of organic matter (OM) from land to ocean is a significant CO_2 sequestration mechanism (e.g., Hedges et al., 1997; Zonneveld et al., 2010; Sinninghe Damsté, 2016). Assessment of OM sources in marine sediments is thus essential to fully comprehend the global carbon cycle. Coastal areas with high riverine inputs are key sites to OM burial in marine environments (e.g., Hedges et al., 1997; Zonneveld et al., 2010) and tropical rivers typically carry a high particulate load and thus OM (e.g., Schlesinger and Melack, 1981; Sinninghe Damsté, 2016). Caribbean and Pacific rivers of Colombia exhibit very high sediment yields due to interplay of high runoff, steep catchments, low variability in annual discharge, episodic sediment delivery associated with geological events (mainly earthquakes), climatic anomalies, such as ENSO, and high rates of deforestation (Table 1; Restrepo and Alvarado, 2011). This makes the coastal areas of Colombia an ideal setting to study terrestrial inputs associated with river discharges. Additionally the present contrasting characteristics allow us to understand the role of climate, geology and hydrology on OM transport.

The origins of OM in marine sediments are multiple and encompass eolian, riverine and runoff discharge as well as production in rivers, marine water column and marine sediments themselves (e.g., Hedges et al., 1997). Both allochthonous and autochthonous OM can also be

* Corresponding author. Geoscience Department, Office M1-305, Los Andes Univeristy, Carrera 1, #18A-12, 111711, Bogotá, Colombia.
** Corresponding author.
E-mail addresses: m.huguet@uniandes.edu.co (C. Huguet), jhkim123@kopri.re.kr (J.-H. Kim).

https://doi.org/10.1016/j.jsames.2019.102349
Received 10 July 2019; Received in revised form 3 September 2019; Accepted 3 September 2019
Available online 10 September 2019
0895-9811/

Table 1
Descriptive parameters for the main rivers in the study area. Parameters are length (L), catchment area (C), slope (S) calculated as the ratio between maximum height and length, average discharge (Qav.) and annual sediment yield (Y). Modified from Restrepo and Alvarado (2011).

	L (km)	C (km^2)	S (%)	$Q_{av.}$ ($m^3\ s^{-1}$)	Y ($t\ km^{-2}\ yr^{-1}$)
Pacific Coast					
Mira	317	9530	1.56	868	1018
Patía	415	23,700	1.10	1490	1500
San Juan	352	16,470	1.11	2550	1150
Caribbean Margin					
Atrato	700	35,700	0.45	2740	815
Sinú	300	14,700	1.12	373	589
Magdalena	1612	257,440	0.20	7232	560

transported laterally by ocean currents. Natural sources of OM can be further distinguished from petroleum-related OM; petrogenic organic carbon (OC) will have a strong impact on natural environments affecting not only local and regional communities, but the whole food web and ultimately the overall equilibrium of the carbon cycle.

In the present study we use of biomarkers and their ratios to obtain information on the transport and deposition of different OM sources. Originally, branched glycerol dialkyl glycerol tetraethers (brGDGTs) were thought to be exclusively produced by soil bacteria, and were then used to derive terrestrial temperature and pH (e.g., Weijers et al., 2007; Schouten et al., 2013). While they have been postulated to be produced by Acidobacteria (Sinninghe Damsté et al., 2011, 2014), the specific source has so far not been identified. Initially described as nine chemical structures (e.g., Weijers et al., 2007) it was recently discovered that most of those present isomers, and that the relative abundance of the isomers is dependent on the brGDGTs origin (de Jonge, 2014, De Jonge et al., 2015). These compounds were used to define a whole suite of new indices, helping discriminate between different sources of OM (e.g., Sinninghe Damsté, 2016). Crenarchaeol is an Archaea membrane isoprenoid GDGT, and in contrast to the brGDGTs, one of isoprenoid GDGTs (isoGDGTs), can be directly linked to nitrifying Archaea belonging to the Thaumarchaeota group (e.g., Sinninghe Damsté et al., 2002). It has thus been used as the marine end member for the Branched versus Isoprenoid tetraether (BIT) index, a proxy of terrestrial soil input (see Hopmans et al., 2004 for details).

An additional type of lipids, *n*-alkanes, are leaf waxes and as such, insoluble, present low volatility, and are resistant to biodegradation making them excellent biomarkers. The *n*-alkanes can be eroded from leaf surfaces by wind so they can be transported, however very often they will be washed out by rain and transported to the ocean by rivers instead (e.g., Eglinton and Eglinton, 2008). The *n*-alkanes can range from 15 to 40 carbons and natural alkanes will be mainly odd numbered, while petrogenic ones will be even numbered. The different chain lengths are depending on their source organism, with shorter *n*-$C_{15\text{-}19}$ belonging to aquatic plants and *n*-$C_{25\text{-}35}$ to higher terrestrial plants (e.g., Brassell et al., 1978). The *n*-alkanes are also major components of petroleum (e.g., Brassell and Eglinton, 1980; Eglinton and Eglinton, 2008) and thus they were used to measure petrogenic origin in the marine sediments.

Understanding the complex mixture of OM in terms of its origins and transport mechanisms is the target of the present study. Here we present results from surface sediments taken from the southern Caribbean Sea and the eastern tropical Pacific (Equator–16°N, and 62°W–85°W, Fig. 1) in order to understand the terrestrial and marine influence on coastal environments with different physico-chemical characteristics. We use biomarkers of both bacterial and archaeal origin, brGDGTs and isoGDGTs, respectively (Schouten et al., 2013 and references therein) as well as *n*-alkanes (e.g., Brassell and Eglinton, 1980; Eglinton and Eglinton, 2008) to assess terrestrial OM inputs and marine productivity in two contrasting study areas.

2. Material and methods

2.1. Study area

The study area is in northwestern South America and comprises both the eastern tropical Pacific and the southern Caribbean coasts off Colombia. This is an area with complex climatological setting, differential terrestrial input and contrasting marine systems (Poveda et al., 2006). The hydro-climatology of the area is dominated by seasonal latitudinal shifts in the Intertropical Convergence Zone (ITCZ) responsible for a bimodal rainfall pattern that regulates the dynamics of main drainage basins (Poveda et al., 2006). Additionally, mesoscale atmospheric features such as the Caribbean and the Chocó low-level jets, transport large amounts of water vapor, which modify the rainfall and wind patterns creating a salinity gradients between the Pacific and the Caribbean waters (Poveda et al., 2014). The study area presents six main rivers, three in each marine basin (Fig. 1). The rivers exhibit very different characteristics in the two sides, the Pacific rivers being generally shorter, steeper and with very high discharges relative to their size (Table 1). Meanwhile rivers in the Caribbean are longer and have larger catchment areas, but the sedimentary yields are smaller than the ones in the Pacific (Table 1).

In the Caribbean coast, the Caribbean jet carries moisture away from the Colombian coast and across the Panama Isthmus supporting a marked precipitation gradient along the coast with annual rates ranging from 250 mm in the northernmost Guajira peninsula to ca. 2000 mm in the limits with Panama (Whyte et al., 2008; Poveda et al., 2014). In the Pacific, the Chocó low-level jet (Fig. 1) has the opposite effect, pushing warm moist air masses towards the western Cordillera where they are uplifted and cooled (Poveda et al., 2006), resulting in much higher precipitation.

The average precipitation in the pacific region is 5000 mm per year but it can reach values of up to 12,000 mm per year in certain areas (Álvarez-Villa et al., 2011). Associated to the Chocó stream and the ocean circulation in the area, two main upwelling areas are located in the eastern side of the Pacific coast (orange shaded areas; Fig. 1) with peaks of production in March and November. This is coupled to enhanced primary production due to high nutrient inputs (Rodriguez-Rubio and Stuardo, 2002). The southern Caribbean experiences strong seasonal upwelling (orange shaded area; Fig. 1) from January to May coupled to strong westerly winds (Rueda-Roa and Muller-Karger, 2013). Colombia has five major seaports, four in the Caribbean and one in the Pacific, which are indicated by stars in the map (Ministerio de Industria y turismo, 2013, Fig. 1). In terms of anthropogenic activity and ship transit, the Caribbean vastly surpasses the Pacific coast.

2.2. Sample extraction and purification

A total of 25 core top samples were used in present study; 14 in the Pacific coast and 11 in the Caribbean coast (Fig. 1). Details of sample code, sample name (ID), sample location, depth and repository where they were obtained from, can be found in Table S1. Sediment samples were freeze dried, ground with a pestle and mortar, weighted and placed in 8 ml glass vials. A mixture of 250 μg 5-α-androstane and 1000 μg of C_{46} GDGTs per 100 μl was added to the samples, as internal standards for the quantification of *n*-alkanes and GDGTs, respectively (see Huguet et al., 2006 and Kim et al., 2017 for details). Samples were extracted using dichlormethane (DCM): Methanol (MeOH) (2:1, V:V). Solvent was added in a proportion of 2 vol per volume of sediment sample, sonicated for 15 min and centrifuged for 2 min at 2500 rpm, and then the supernatant was collected with a glass pipette and placed in a glass vial for further processing. The extraction cycle was repeated 3 times. During the last cycle sonication was reduced to 5 min. The total lipid extracts obtained were then dried under N_2 to start fractionation.

Samples were fractioned over a silica column using solvents of increasing polarity. Fraction 1, which includes *n*-alkanes, was separated

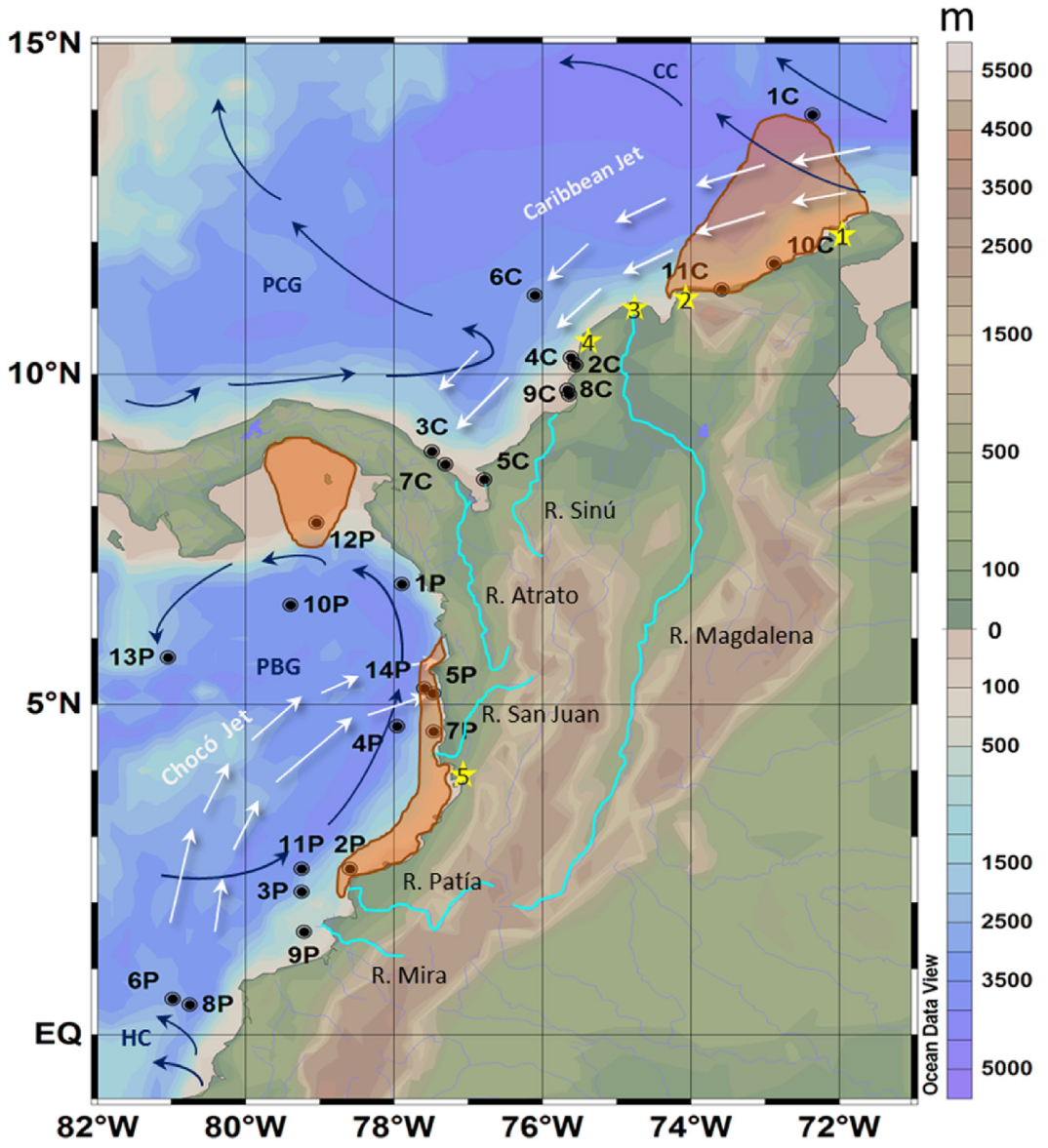

Fig. 1. Map showing the study area with sample locations and main ocean currents (blue arrows) and air streams (White arrows): HC (Humbolt Current), PBG (Panama Bight Gyre), PCG (Panama Colombia Gyre), CC (Caribbean Current). Main harbors are indicated by yellow stars as 1-Puerto Bolivar, 2-Puerto de Santa Marta, 3-Puerto de Barranquilla, 4-Puerto de Cartagena and 5-Puerto de Buenaventura. Shaded orange areas indicate main upwelling areas. Main rivers have been highlighted in light blue. Plot modified from OceanDataView. (For interpretation of the references to colour in this figure legend, the reader is referred to the Web version of this article.)

using hexane. Fraction 2, containing alkenones, was separated using hexane:DCM (1:1, V:V). Finally fraction 3, containing sterols, diols and GDGTs, was separated using DCM:MeOH (1:1; V:V). Fraction 1 was then transferred to GC glass vials and diluted in hexane before injection to measure *n*-alkanes (e.g. Kim et al., 2017). Fraction 3 was dissolved in hexane:isopropanol (99:1; V:V) and filtered through a 0.45 µm PTFE filter and placed in glass vial for analysis of GDGTs (e.g. Huguet et al., 2010).

2.3. Measurements of glycerol dialkyl glycerol tetraethers

The polar fraction was analyzed for GDGTs using an Agilent 1260 UHPLC coupled to a 6130 quadrupole MSD high performance liquid chromatography-atmospheric pressure chemical ionization-mass spectrometry (HPLC-APCI-MS) using a method enabling the separation of 5- and 6-methyl brGDGTs (Hopmans et al., 2016). To improve separation, two UHPLC silica columns (BEH HILIC columns, 2.1, 150 mm, 1.7 l mm; Waters) in series, fitted with a 2.1, 5 mm pre-column of the same material (Waters) were used. Detection was via selected ion monitoring (SIM; Schouten et al., 2013) using *m/z* 744 for the internal standard, *m/z* 1302, 1300, 1298, 1296, and 1292 for isoprenoid GDGTs including crenarchaeol and *m/z* 1050, 1048, 1046, 1036, 1034, 1032, 1022, 1020 and 1018 for brGDGTs. Agilent Chemstation software was used to integrate peak areas in the mass chromatograms of the $[M + H]^+$ ions. Concentrations of GDGTs were calculated using the known concentration of the internal standard (c.f. Huguet et al., 2006) and assuming a similar mass spectrometric response for the isoprenoid and branched GDGTs measured. The GDGTs were also used to calculate ratio to estimate the amount and origin of terrestrial input as shown below. We used a range of indices to evaluate the distribution of brGDGTs based on their fractional abundance (indicated by using square brackets). The roman numbers refer to the different structures found in Fig. S1. The BIT index (Hopmans et al., 2004) was calculated with the inclusion of 6-methyl brGDGTs (De Jonge et al., 2014) as:

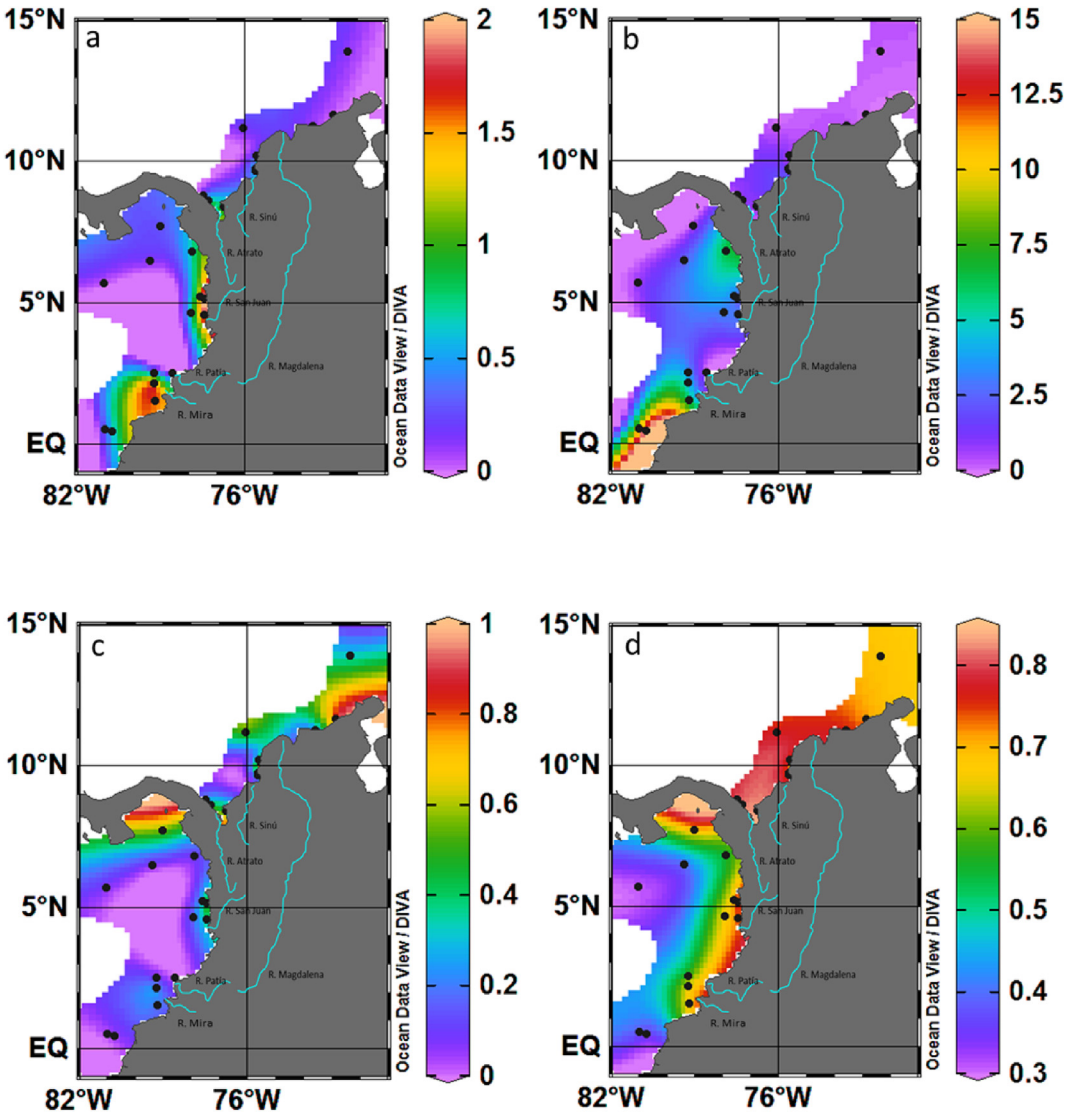

Fig. 2. Spatial distribution of biomarkers in sediments for a) acyclic brGDGTs (μg/g_{sed}), b) crenarchaeol (μg/g_{sed}), C) BIT index, and D) #$Rings_{tetra}$. Main rivers have been indicated in light blue. (For interpretation of the references to colour in this figure legend, the reader is referred to the Web version of this article.)

$$BIT = \frac{Ia + IIa + IIIa + IIa' + IIIa'}{Ia + IIa + IIIa + IIa' + IIIa' + IV} \quad (1)$$

The index of $\#rings_{tetra}$ (Sinninghe Damsté, 2016) was calculated as an indication of sediment in situ production of brGDGTs, as follows:

$$\#rings_{tetra} = \frac{[Ib] + 2 \times [Ic]}{[Ia] + [Ib] + [Ic]} \quad (2)$$

2.4. Measurements of saturated hydrocarbons

The *n*-alkanes in the saturated hydrocarbon fraction were identified with a Shimadzu GC-2010 gas chromatograph interfaced to a Shimadzu GCMS-QP2010 plus using a DB-5 fused silica capillary column (30 m, 0.25 mm, film thickness of 0.25 mm, J&W Scientific) with helium as a carrier gas. Mass scans were made in the range of m/z = 40–600 with 0.1 scan per second and an ionization energy of 70 eV. Samples were injected in the splitless mode. The temperature for both the injector and the detector was 310 °C. The oven program initiated at 70 °C and increased at a rate of 20 °C/min to 130 °C and subsequently by a rate of 4 °C/min until 320 °C. The final temperature of 320 °C was held for 25 min. Compound identifications were based on a comparison of relative GC retention times and mass spectra of the *n*-alkane mixture (*n*-C_8-C_{40}) analytical standards (Supelco 502065, AccuStandard, USA). The *n*-alkane peaks with carbon lengths from C_{15} to C_{35} were integrated using Agilent Chemstation software (Kim et al., 2017). The *n*-alkane absolute abundances were calculated relative to the internal standard 5-α-androstane and then normalized to grams of sediment since no TOC data was available. The abundance of odd *n*-$C_{15\text{-}19}$ as indicator of aquatic production and odd *n*-$C_{25\text{-}35}$ as marker for higher plants was calculated. Additionally a series of indices using *n*-alkanes were calculated to estimate the amount and type of terrestrial input. The average chain length (ACL; e.g., Cranwell, 1984):

$$ACL = \frac{25 \times C_{25} + 27 \times C_{27} + 29 \times C_{29} + 31 \times C_{31} + 33 \times C_{33}}{C_{25} + C_{27} + C_{29} + C_{31} + C_{33}} \quad (3)$$

The carbon preference index (CPI, Bray and Evans, 1961) was calculated using alkanes from 25 to 35 carbons as follows:

$$CPI = \frac{1}{2} \times \left[\left(\frac{C_{25} + C_{27} + C_{29} + C_{31} + C_{33}}{C_{24} + C_{26} + C_{28} + C_{30} + C_{32}} \right) + \left(\frac{C_{25} + C_{27} + C_{29} + C_{31} + C_{33}}{C_{26} + C_{28} + C_{30} + C_{32} + C_{34}} \right) \right] \quad (4)$$

2.5. Statistical analyses

The fractional abundances of brGDGTs (Ia-IIIc) and *n*-alkane (*n*-C_{15}-C_{35}) compounds were obtained by normalizing each concentration to the summed concentration of all homologues considered (Appendix Tables S2 and S3). Principal Component Analysis (PCA) was performed on the fractional abundance to provide a general view of the variability of the distribution of brGDGTs and *n*-alkanes by using the R program (Pinheiro et al., 2015).

3. Results

3.1. Biomarker abundances

A clear difference is observed not only on terrestrial matter inputs but also in the production of the two studied basins. Biomarker concentrations are overall higher in the Pacific with values up to one order of magnitude greater. Higher acyclic brGDGT concentrations, related to soil input, were found in the Pacific coast related to river outlets, and lower values are measured in offshore Caribbean (Fig. 2a).

Acyclic brGDGTs ranged between 0.04 and 1.0 μg/g_{sed} in the Caribbean (Figs. 2a) and 0.1–2.4 μg/g_{sed} in the Pacific (Fig. 2a). Crenarchaeol concentrations, which would indicate marine Archaea production, are also higher in the Pacific (ranging from 0.2 to 14.2 μg/g_{sed}; Fig. 2b) than in the Caribbean (ranging from 0.006 to 1.8 μg/$g_{sed.}$; Fig. 2b). Unlike the terrestrial input, crenarchaeol concentrations are highest in the southernmost samples and station P1 both in the Pacific (Figs. 1 and 2b).

The odd numbered *n*-$C_{25\text{-}35}$ *n*-alkanes, also used as a terrestrial input marker, ranged from 0.6 to 3.6 μg/g_{sed} in the Caribbean, reaching much higher values 0.7–13.7 μg/g_{sed} in the Pacific (Fig. 3a) confirming the acyclic brGDGT distribution. The odd numbered *n*-alkanes *n*-$C_{15\text{-}19}$ concentrations, which indicate algal and photosynthetic bacteria in situ production, were between 0.04 and 4.1 μg/g_{sed} and between 0.3 and 7.9 μg/g_{sed} in the Pacific (Fig. 3b). In the case of the *n*-alkanes the two ranges displayed contrasting patterns with higher continental input detected offshore and increased algal production closer to the coast (Fig. 3a and b). In contrast, the Caribbean presents lower biomarker abundances even in stations close to the coast (Figs. 2a and 3a).

3.2. Indices of terrestrial input and in situ production

With the exception of site 12P the BIT index was lower in the Pacific than in the Caribbean (Fig. 2c). Pacific BIT values diminish from coastal to more open sea samples, with more terrestrial signal associated to the major rivers in that coast. In the Caribbean instead highest BIT index in station 10C is not associated to a river outlet (Figs. 1 and 2c). However, BIT values higher than 0.5 are observed in the Gulf of Urabá where the Atrato River discharges (Figs. 1 and 2c). In the case of the #$rings_{tetra}$ highest values can be seen in the Caribbean with all values above 0.7 (Fig. 2d). In the Pacific a clear decrease of the #$rings_{tetra}$ is observed as we move further away from the coast, with coastal values up to 0.9 and decreasing to 0.3 in the more open water locations (Fig. 2d).

The ACL index ranges between 28.5 and 31, with highest values found in the Pacific (Fig. 3c). While station 10P shows a value of 31 ACL, all other stations are below 30, with the lowest values found in the Caribbean Coast (Fig. 3c). The CPI values were generally higher in the Pacific, with very few points approaching zero (Fig. 3d). Lower CPI values were found in samples close to the coast in some cases related to the presence of harbors (Figs. 1 and 2d).

3.3. PCA results and cluster analysis

The principal component analysis of the 15 brGDGTs shows a component 1 that explained 61.6% of the variation and a component 2 that explained 13.9 (Fig. 4a). According to these components, samples can be divided in 3 clusters, 1 and 2 that separate according to component 2 and Cluster 3 separated from the other two in the X axis (Fig. 4b).

Clusters 1 and 2 plot closer to the coast, while cluster 3 is only found in more open water samples of the Pacific (Fig. 4c). While brGDGTs distributions in cluster 1 and 2 mainly differ in the dominance of Ia (Cluster 2) versus abundance of Ib and Ic (Cluster 1), Cluster 3 presents a very different distribution (Fig. 4d).

In the case of the PCA of *n*-alkanes the first component explains 46.1% and the second 22.6% of the variation (Fig. 5a). According to this components stations plot in 4 clusters, mainly related to the quadrants of the PCA (Fig. 5b). Cluster 1 includes the lowest *n*-alkane chain lengths and Cluster 3 the highest, with Cluster 4 being the most different (Fig. 5). Cluster 1 is usually found further away from the coast while others are closer (Fig. 5c). Cluster 4 can only be found in 2 samples of the Caribbean followed in size by Cluster 2 that only includes 3 samples, 2 in the Pacific and 1 in the Caribbean (Fig. 5c). Clusters 1 and 2 show a predominance of low chain *n*-alkanes (highest values of *n*-C_{18}) and Clusters 3 and 4 display higher n-alkane chains (highest values *n*-C_{31}; Fig. 5d).

4. Discussion

The two study areas present strong contrast both on OM terrestrial input and marine production, with the Pacific presenting higher values for both parameters. The Colombian Pacific coast is characterized by dense tropical rain forests, active fault systems, steeper slopes and high precipitation rates (with some areas reaching up to 12,000 mm annually; Aalto et al., 2006; Poveda et al., 2014) and it has already been described to have higher inorganic sedimentary loads (Restrepo and Alvarado, 2011). The Caribbean basin is instead oligotrophic mainly because it has smaller and seasonal upwelling cells, receives less precipitation, and extensive river floodplains act as sedimentary traps, and thus a smaller inorganic sedimentary load reaches coastal waters (Rodriguez-Rubio and Stuardo, 2002; Rueda-Roa and Muller-Karger, 2013; Poveda et al., 2014) all of which result in less nutrients present in the system and thus diminished in situ production. The aim of the paper was to analyze the sources, modes of delivery and storage and degradation of OM in the two contrasting coasts and will be discussed in detail in the following sections.

4.1. Source of biomarkers

There are two main natural sources for the biomarkers in this study, continental soil and vegetation input, and in situ production in the water column or sediments. While we tried to quantify terrestrial organic input using the BIT index (Hopmans et al., 2004; De Jonge et al., 2014), since crenarchaeol concentrations are up to three times higher than brGDGTs (Fig. 2), values were dominated by in situ Thaumarchaeota production rather than continental input. Problems with the use of the BIT index in relation to biomarker concentrations have been previously reported (e.g., Fietz et al., 2011a; Smith et al., 2012).

Using the #$ring_{tetra}$ (Sinninghe-Damsté, 2016) we observe the prevalence of in situ production of brGDGTs at the Caribbean side while only a few coastal stations in the eastern Pacific present values higher than 0.7 and thus transport of brGDGTs from soils. This would further explain the lack of correlation between other terrestrial input indicators

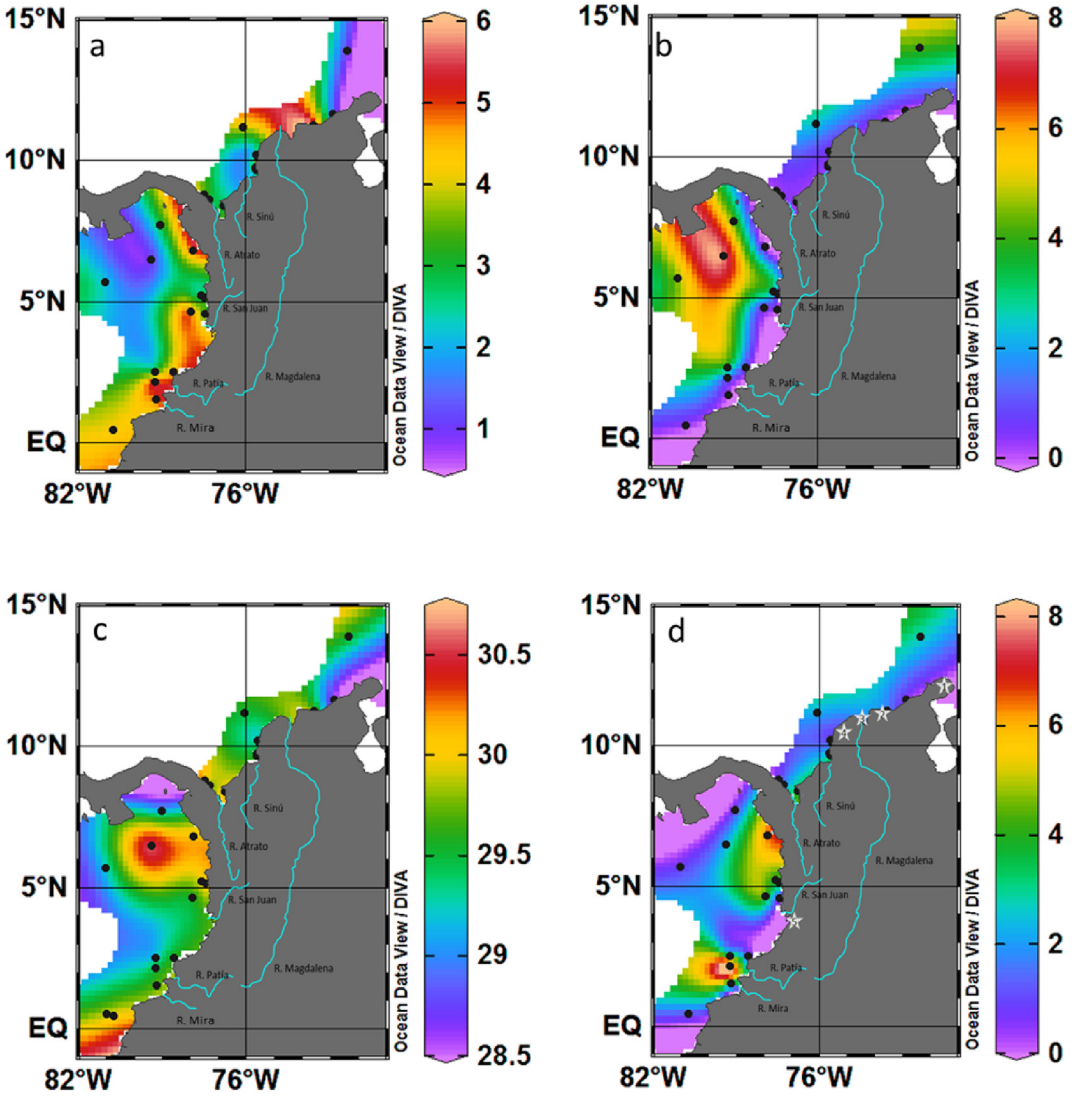

Fig. 3. Spatial distribution of biomarkers in sediments for a) odd numbered *n*-alkanes *n*-$C_{25\text{-}35}$ (μg/g_{sed}), b) odd numbered *n*-alkanes *n*-$C_{15\text{-}19}$ (μg/g_{sed}), c) ACL, and d) CPI (*n*-$C_{25\text{-}35}$). Main rivers have been indicated in light blue and harbors with grey stars. (For interpretation of the references to colour in this figure legend, the reader is referred to the Web version of this article.)

and BIT values since in situ production of both BIT endmembers is taking place (e.g., Fietz et al., 2011a, 2011b and references therein).

We thus used acyclic brGDGTs concentrations as indicators of soil terrestrial input. They were found to be elevated in coastal areas associated mainly to river mouths in the Pacífic. This terrestrial input indicator matches known inorganic terrestrial inputs (Rodriguez-Rubio and Stuardo, 2002; Rueda-Roa and Muller-Karger, 2013; Poveda et al., 2014) as well as *n*-alkane distributions of higher plants in the present study. There is a predominance of acyclic brGDGT Ia especially in the more coastal samples of clusters 1 and 2. High Ia in tropical soils is explained by both the low pH that results in the dominance of acyclic GDGTs and the low degree of methylation associated to higher tropical temperatures. While cluster 1 has elevated Ia, it contains a higher proportion of Ib and Ic, indicating a higher degree of cyclisation and thus higher pH in the Caribbean. This may be due to more basic soils being washed in the Caribbean area but we think instead it is reflecting the more basic conditions found in the Caribbean basin itself (e.g. Molnar, 2008; Poveda et al., 2014), since in situ acyclic brGDGT production is high in that area. Cluster 3 with higher proportions of cyclized and methylated brGDGTs is only found in the Pacific. The stations in the cluster are also the ones that show the highest # $ring_{tetra}$ and thus would be indicating the transported continental soil signal without overwriting from in situ brGDGT production in the sediments. They are also the deeper stations in the dataset so a better preservation of the signal could also take place.

Terrestrial plant input, as recorded by long chain odd n-alkanes, is also higher in Pacific thus confirming that organic input is coupled to inorganic matter contribution patterns. Coastal stations in both the Caribbean and Pacific are clearly dominated by *n*-C_{29}, *n*-C_{31}, and *n*-C_{33} (Cluster 3, Fig. 5), indicating that the main source of hydrocarbons is continental vegetation. Only three samples fall within cluster 4 that shows not only high values of *n*-C_{29}, *n*-C_{31} and *n*-C_{33}, but also elevated *n*-C_{21}, *n*-C_{23} and *n*-C_{25} abundances. Odd numbered mid-molecular weight *n*-alkanes with maximum in *n*-C_{21}, *n*-C_{23} and *n*-C_{25} are indicators of freshwater and submerged macrophytes (e.g., Ficken et al., 2000; Mead et al., 2005). All stations in cluster 4 are at the Caribbean coast (Fig. 5) and their natural hydrocarbon distribution could be related to coastal vegetation such as mangroves that can be found in the area (González et al., 2006). As *n*-alkane distributions for *Rhizophora mangle* (Red Mangrove) show increasing abundances from C_{23} to C_{29} (Mead et al., 2005), based on that, this vegetation type can be ruled out as a source of the observed signal. The ACL index (e.g., Cranwell, 1984) has been related to the type of terrestrial vegetation where the *n*-alkanes come from, with C_3 plants showing a ACL of 29 and C_4 grasses

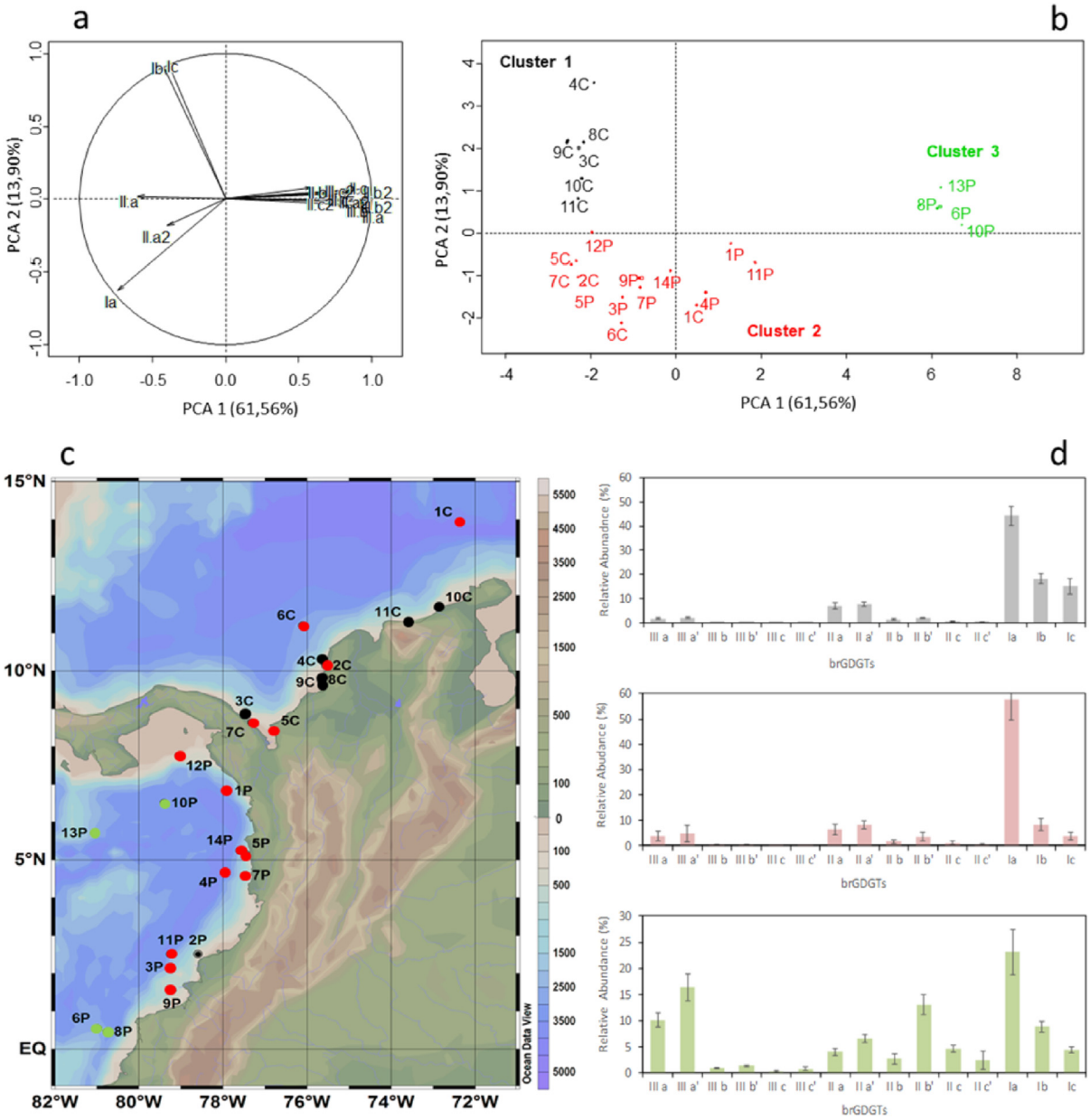

Fig. 4. Results of (a) the Principal Component Analysis (PCA) and b) Hierarchical Clustering on Principal Components (HCPC) based on the fractional abundance of the 15 brGDGTs compounds, c) map showing the spatial distribution patterns of 3 clusters obtained from the HCPC, and d) average brGDGTs distributions of the corresponding clusters. Roman numerals refer to the structure of brGDGTs (see Appendix Fig. S1).

displaying higher ACL vales around 30.7 (e.g., Bianchi and Canuel, 2011; Rommerskirchen et al., 2006). All the ACL values measured are below 30.7, so no overall dominance of C_4 plants in either basin. However, some stations at the Caribbean and half the stations at the Pacific (to the north) display values around 30 indicating a significant C_4 grass signal. This is most likely related to the dominance of more arid and open ecosystems in the Caribbean, and to the trajectory of the Caribbean low-level jet that carries plant remains from northern South America and deposits them in the northern corner of the tropical Pacific.

In situ primary production is higher in the Pacific, coupled to higher terrestrial and hence nutrient input. While stations far away from the coast are dominated by in situ production they still record a continental vegetation signal. The odd short chain *n*-alkanes (n-$C_{15\text{-}19}$) have been used to evaluate algal and/or bacteria productions (e.g., Han and Calvin, 1969; Meyers and Ishlwatari, 1993, Fig. 3b). Highest production was found in coastal Pacific stations with concentrations above 6 μg/g_{sed} in some samples. High algal and/or bacterial production are associated to riverine inputs but also show a good correspondence with upwelling systems (Figs. 1 and 3b). The primary production as indicated by short chain *n*-alkanes is associated mainly to one of the upwellings in the area (Fig. 1) which is also reported to display high chlorophyll levels (Rodriguez-Rubio and Stuardo, 2002). Like riverine discharge, upwelling will increase the amount of nutrients in the water column and hence foster higher levels of primary production. At the Caribbean side, higher values are close to the mouth of the Magdalena River and at the Gulf of Urabá in the Panama border (outlet of the Atrato River) most likely associated with high particulate loads and thus nutrient levels (Rodriguez-Rubio and Stuardo, 2002; Rueda-Roa and Muller-Karger, 2013; Poveda et al., 2006, 2014). However, like in the Pacific, stations C10 and C11 may also be influenced by the seasonal upwelling present in that area (Figs. 1 and 3b).

We evaluated the crenarchaeol concentrations as indicator of nitrifying Archaea belonging to the Thaumarchaeota group (e.g.,

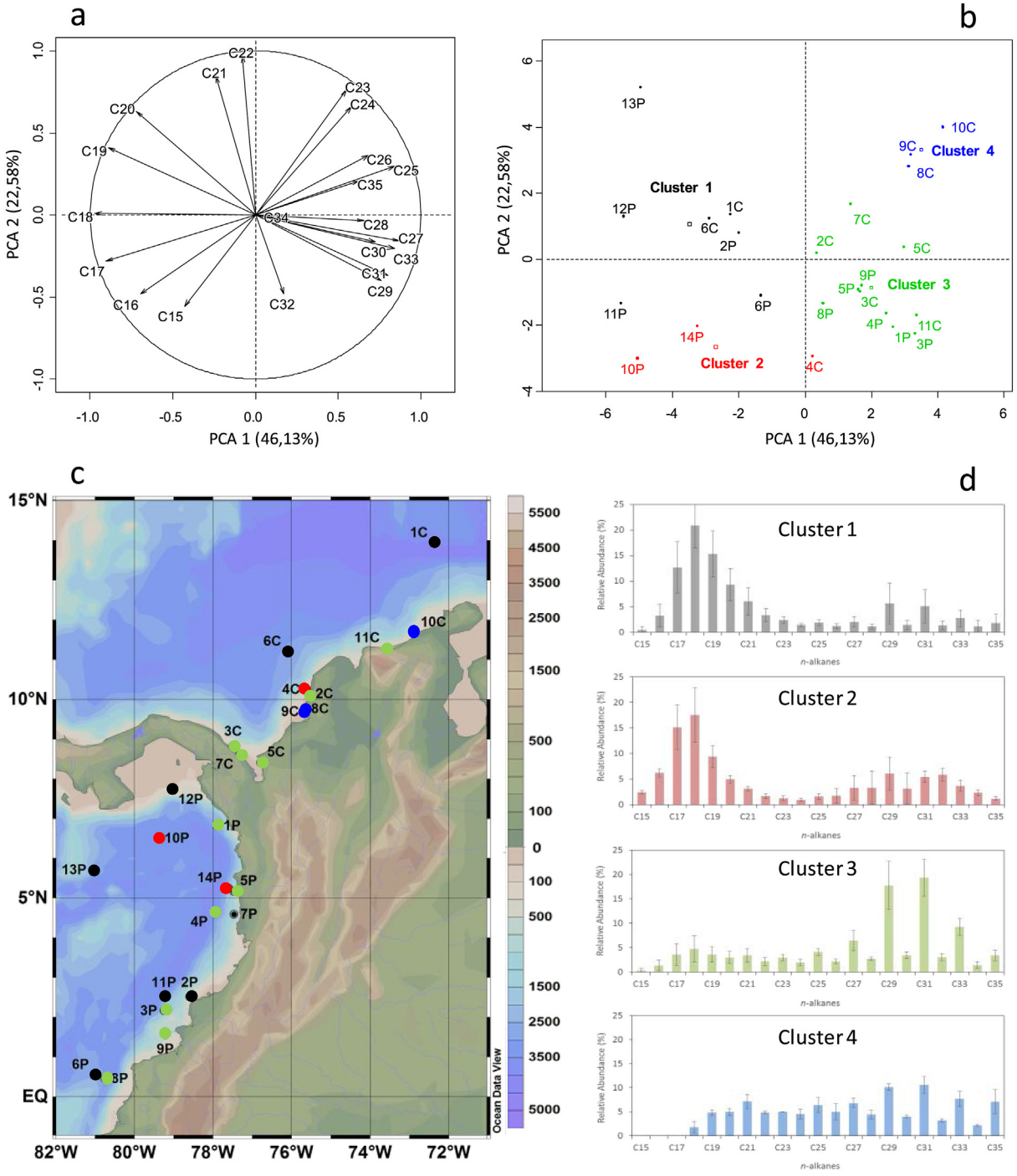

Fig. 5. Results of (a) the Principal Component Analysis (PCA) and b) Hierarchical Clustering on Principal Components (HCPC) based on the fractional abundance of *n*-alkanes *n*-$C_{15\text{-}35}$, c) map showing the spatial distribution patterns of 4 clusters obtained from the HCPC, and d) average *n*-alkanes distributions of the corresponding clusters.

Sinninghe Damsté et al., 2002). Thaumarchaeota have been found to dominate coastal nitrification (e.g. Urakawa et al., 2014). A good correlation was reported between intact isoprenoid GDGTs (including crenarchaeol) and ammonia oxidation rates (Urakawa et al., 2014). Crenarchaeol concentrations were found to be up to eight times higher in the Pacific, in agreement with the nitrate concentrations (Fig. 1S). Highest values in the Pacific were found close to the equator probably related to nutrient-rich waters carried by the Humboldt Current (Fig. 1) from the Peru upwelling area. High crenarchaeol and nitrate are also coupled to the Pacific Upwelling and input of the San Juan River (Figs. 1 and 1S). Overall, nitrate and crenarchaeol concentrations were low in the Caribbean even in coastal or riverine input areas. While a crenarchaeol and phytoplankton abundance coupling has been observed in several study areas (Fietz et al., 2011b) this is not the case for the present study.

4.2. Delivery mode of terrestrial OM into coastal environments

The two main ways of transport of terrestrial OM to the marine environment are eolian transport and water discharge either through rivers or surface runoff. In order to disentangle the two, we used acyclic brGDGTs mainly as riverine discharge indicators and *n*-alkanes as

eolian input tracers, however, when we compare Figs. 2a and 3a we observe similar distributions. Which could indicate, despite our initial premise of differential delivery systems, both enter the ocean through the same mechanism. Concentration of both are higher in river mouths especially the Mira and Patia rivers at the Pacific Coast (Figs. 1 and 2a) which would point to this as the main delivery mechanism for *n*-alkanes and brGDGTs. However, stations north of the San Juan River also present high brGDGTs and that may be related to either smaller rivers in the area, and/or surface runoff (Figs. 1 and 2a). That coastal area receives moisture pushed inland by the Chocó jet (Fig. 1) which is then uplifted and cooled resulting in the Chocó being one of the wettest places on Earth (annual average can be as high as 12,000 mm). High precipitation coupled to the steepness of the terrain favors the formation of short rivers that discharge great amounts of water, resulting in great denudation and erosion (Restrepo and Kjerfve, 2000; Restrepo and Alvarado, 2011). Thus, even though rivers are shorter and present smaller catchments, the sedimentary loads are highest in the Pacific region (Table 1; Restrepo and Alvarado, 2011) validating our biomarker distributions. The same could explain the elevated *n*-alkanes of higher plants (*n*-$C_{25\text{-}35}$) in station P10 (Figs. 1 and 3a). However, since continental *n*-alkanes can also be transported via eolian dusts (e.g., Brassell and Eglinton, 1980; Eglinton and Eglinton, 2008), the winds from the Caribbean low-level jet should not be ruled out as a possible transport mechanisms in this particular case. Especially since the ACL indicates a drier signal in the stations of the north tropical Pacific. Another way to explain the high concentration of *n*-alkanes in station P10 would be related to the Panama Bight Gyre (Fig. 1) funneling biomarkers to that specific location. This latter hypothesis is supported by stations P12 and 13 (Fig. 1) also having elevated *n*-$C_{25\text{-}35}$ *n*-alkane concentrations (Fig. 3a).

In the Caribbean, we observe higher acyclic brGDGT abundances in the Urabá Gulf, bordering Panama, as compared to the Magdalena or de Sinú discharge areas (Figs. 1 and 2a). This might be because sampling resolution does not allow for a one to one comparison, but also because the Atrato River drains one of the wettest catchments in the Pacific, but flows into the Caribbean. This hypothesis is supported by the Atrato River delivering the highest sediment yields in the Caribbean area (Table 1; Restrepo and Alvarado, 2011). The *n*-alkanes of higher plants are highest in station 1C (Fig. 1), and since this station is off shore this is likely not related to either eolian or riverine input. Instead, we believe that the high *n*-alkane values are related with the influx of the Caribbean Current (Fig. 1) bringing water masses from further south with a higher biomarker load.

4.3. Petrogenic signal

Petroleum is a complex mixture of many organic compounds, which includes preferentially even numbered *n*-alkanes (e.g., Bianchi and Canuel, 2011; Wang et al., 1999). Hydrocarbons of petroleum origins enter the system through anthropogenic processes such as shipping activity or industrial dumping (e.g., Wang et al., 1999; Kim et al., 2017). Overall petrogenic contamination was higher in the Caribbean than in the Pacific due most likely to increased activity in that basin. The CPI (Bray and Evans, 1961) was calculated to estimate petroleum inputs into the sediments with expected values above 4 for natural sources and values of 1 or lower for petrogenic *n*-alkanes (e.g., Simoneit, 1984). Higher CPI values are found in the Pacific than in the Caribbean (Fig. 3d) indicating less inputs of petroleum-derived *n*-alkanes into that basin. Nonetheless stations 2P, 7P, 12P and 13P display CPI values below 2 that indicate some petrol contamination (Figs. 1 and 3d). Station 7P is close the Buenaventura Harbour (Fig. 1) with a transport activity above 12.1 Millions of Tons (MT; Ministerio de Industria y Turismo, 2013) that would explain elevated petrol concentrations in the sediments. In the case of station 2P (Fig. 1), low CPI values could be related to petrol-contaminated waters from the Patia River. The other stations may be explained either by dumping of petrol form Central American harbors, due to recirculation of water masses in the Panama Bight Gyre or re-working of sediments by bottom currents.

In the Caribbean, we find values of CPI below 1 in some coastal stations, especially those related to main seaports (Fig. 1) and 1 at the Gulf of Urabá. Not only the Caribbean has higher number of harbors but also they have much higher activity than the Buenaventura one (Ministerio de Industria y Turismo, 2013) thus explaining lower CPI values in that basin. Regarding the Gulf of Urabá (covered in our study by samples 3C, 5C and 7C; Fig. 1) a previous study reported surface sediments contamination with Zn (from pesticides) and Ag (from mining activity in the area) (Toro et al., 2016). While the Gulf of Urabá presents no harbors, there is very high export shipping activity that takes place off shore (CH personal observation) and could explain low CPI values in our samples.

5. Conclusions

Clear differences can be observed in terms of terrestrial input, marine productivity and diversity between the two study areas highlighting the potential of the multipxoy approach to trace back hydrological changes and weathering over the continental tropical South America as well as its consequences in coastal environments. The Caribbean study area presents smaller sedimentary loads associated with lower nutrient levels, which results in lesser productivity and diversity in the area. In addition to higher sedimentary load, the Pacific side is also influenced by the Humboldt Current, which results in further enhancement of productivity due to nutrient upwelling in that setting compared to the Caribbean. We propose that the main source of terrestrial OM is related to river discharge. Acyclic brGDGT biomarkers are good indicators of terrestrial OM input even though coastal areas, especially the Caribbean one show significant in situ production. The application of *n*-alkanes allowed to distinguish between OM photosynthetic sources and helped confirm mainly riverine continental OM input. Crenarchaeol was highly correlated to nutrient input and nitrate as an end result of Thaumarchaeota ammonia oxidation. Petrogenic contamination was higher at the Caribbean, specially related to main harbors in that area.

Acknowledgements

This work was partially funded by FAPA project “Biomarcadores lípidicos para reconstrucciones paleoclimáticas” [R.3.2015.2423; Los Andes University] to CH. This work was also supported by the National Research Foundation of Korea (NRF) grant funded by the Ministry of Science and ICT [MSIT, No. NRF-2016R1A2B3015388, KOPRI-PN19100] to J-H. K. This project was conceived by CG and CH as part of the project “Distribución de palinomorfos marinos y terrestres en sedimentos marinos superficiales del Mar Caribe y el Pacífico tropical oriental en relación con parámetros ambientales” funded by COLCIENCIAS [project 1204–569–34184]. We are grateful to Centro de Innovación y Tecnología from the Instituto Colombiano de Petróleo (ICP), Laboratorio Biología Marina Uniandes (BIOMAR), Lamont–Doherty Earth Observatory (LDEO), Ocean Drilling Program (ODP, OIDP), and EAFIT University for providing samples.

Appendix A. Supplementary data

Supplementary data to this article can be found online at https://doi.org/10.1016/j.jsames.2019.102349.

References

Aalto, R., Dunne, T., Guyot, J.J., 2006. Geomorphic controls on Andean denudation rates. J. Geol. 114, 85–99.

Álvarez-Villa, O.D., Vélez, J.I., Poveda, G., 2011. Improved long-term mean annual rainfall fields for Colombia. Int. J. Climatol. 31, 2194–2212.

Bianchi, T.S., Canuel, E.A., 2011. Chemical Biomarkers in Aquatic Ecosystems. Princeton University Press, pp. 185–206.
Brassell, S.C., Eglinton, G., 1980. Environmental chemistry-an inter-disciplinary subject. Natural and pollutant organic compounds in contemporary aquatic environments. In: Analytical Techniques in Environmental Chemistry: Proceedings of the International Congress. Pergamon, Barcelona, Spain.
Brassell, S.C., Eglinton, G., Maxwell, J.R., Philp, R.P., 1978. Natural background of alkanes in the aquatic environment. In: Hutzinger, O., van Lelyveld, I.H., Zoetman, B.C.J. (Eds.), Aquatic Pollutants: Transformation and Biological Effects. Pergamon Press, Oxford, pp. 69–86.
Bray, E.E., Evans, E.D., 1961. Distribution of *n*-paraffins as a clue to recognition of source rocks. Geochem. Cosmochim. Acta 22, 2–15.
Cranwell, P.A., 1984. Lipid geochemistry of sediments from Upton Broad, a small productive lake. Org. Geochem. 7, 25–37.
De Jonge, C., Hopmans, E.C., Zell, C.I., Kim, J.-H., Schouten, S., Sinninghe Damsté, J.S., 2014. Occurrence and abundance of 6-methyl branched glycerol dialkyl glycerol tetraethers in soils: implications for palaeoclimate reconstruction. Geochem. Cosmochim. Acta 141, 97–112.
De Jonge, C., Stadnitskaia, A., Hopmans, E.C., Cherkashov, G., Fedotov, A., Streletskaya, I.D., Damsté, J.S.S., 2015. Drastic changes in the distribution of branched tetraether lipids in suspended matter and sediments from the Yenisei River and Kara Sea (Siberia): Implications for the use of brGDGT-based proxies in coastal marine sediments. Geochimica et Cosmochimica Acta 165, 200–225.
Eglinton, T.I., Eglinton, G., 2008. Molecular proxies for paleoclimatology. Earth Planet. Sci. Lett. 275, 1–16.
Fietz, S., Martínez-Garcia, A., Huguet, C., Rueda, G., Rosell-Melé, A., 2011a. Constraints in the application of the Branched and Isoprenoid Tetraether index as a terrestrial input proxy. J. Geophys. Res.: Oceans. https://doi.org/10.1029/2011JC007062.
Fietz, S., Martínez-Garcia, A., Rueda, G., Peck, V.L., Huguet, C., Escala, M., Rosell-Melé, A., 2011b. Crenarchaea and phytoplankton coupling in sedimentary archives: common trigger or metabolic dependence? Limnol. Oceanogr. 56 (5), 1907–1916.
Ficken, K.J., Li, B., Swain, D.L., Eglinton, G., 2000. An *n*-alkane proxy for the sedimentary input of submerged/floating freshwater aquatic macrophytes. Org. Geochem. 31, 745–749.
González, C., Urrego, L.E., Martínez, J.I., 2006. Late Quaternary vegetation and climate change in the Panama Basin: palynological evidence from marine cores ODP 677B and TR 163-38. Palaeogeogr. Palaeoclimatol. Palaeoecol. 234, 62–80.
Han, J., Calvin, M., 1969. Hydrocarbon distribution of algae and bacteria, and microbiological activity in sediments. Proc. Natl. Acad. Sci. 64, 436–443.
Hedges, J.I., Keil, R.G., Benner, R., 1997. What happens to terrestrial organic matter in the ocean? Org. Geochem. 27, 195–212.
Hopmans, E.C., Schouten, S., Sinninghe Damsté, J.S., 2016. The effect of improved chromatography on GDGT-based palaeoproxies. Org. Geochem. 93, 1–6.
Hopmans, E.C., Weijers, J.W., Schefuß, E., Herfort, L., Sinninghe Damsté, J.S., Schouten, S., 2004. A novel proxy for terrestrial organic matter in sediments based on branched and isoprenoid tetraether lipids. Earth Planet. Sci. Lett. 224, 107–116.
Huguet, C., Martens-Habbena, W., Urakawa, H., Stahl, D.A., Ingalls, A.E., 2010. Comparison of extraction methods for quantitative analysis of core and intact polar glycerol dialkyl glycerol tetraethers (GDGTs) in environmental samples. Limnol Oceanogr. Methods 8 (4), 127–145.
Huguet, C., Hopmans, E.C., Febo-Ayala, W., Thompson, D.H., Sinninghe Damsté, J.S., Schouten, S., 2006. An improved method to determine the absolute abundance of glycerol dibiphytanyl glycerol tetraether lipids. Org. Geochem. 37, 1036–1041.
Kim, J.-H., Lee, D.-H., Yoon, S.-H., Jeong, K.-S., Choi, B., Shin, K.-H., 2017. Contribution of petroleum-derived organic carbon to sedimentary organic carbon pool in the eastern Yellow Sea (the northwestern Pacific). Chemosphere 168, 1389–1399.
Mead, R., Xu, Y., Chong, J., Jaffé, R., 2005. Sediment and soil organic matter source assessment as revealed by the molecular distribution and carbon isotopic composition of *n*-alkanes. Org. Geochem. 36, 363–370.
Meyers, P.A., Ishlwatari, R., 1993. The early diagenesis of organic matter in lacustrine sediments. In: Engel, M., Macko, S.A. (Eds.), Organic Geochemistry. Plenum, New York, pp. 185–209.
Ministerio de Industria y turismo, 2013. Puertos Marítimos. http://www.mincit.gov.co/publicaciones/5871/puertos_maritimos_movieron_153_millones_de_toneladas_en_2012.
Molnar, P., 2008. Closing of the central American seaway and the ice age: a critical review. Paleoceanography 23 (2). https://doi.org/10.1029/2007PA001574.
Pinheiro, J., Bates, D., DebRoy, S., Sarkar, D., 2015. R Development Core Team.(2015). nlme: Linear and nonlinear mixed effects models (R package version 3.1-120). http://CRAN.R-project.org/package=nlme.
Poveda, G., Jaramillo, L., Vallejo, L.F., 2014. Seasonal precipitation patterns along pathways of South American low-level jets and aerial rivers. Water Resour. Res. 50, 98–118.
Poveda, G., Waylen, P.R., Pulwarty, R.S., 2006. Annual and inter-annual variability of the present climate in northern South America and southern Mesoamerica. Paleogeogr. Paleoclimatol. Paleoecol 234, 3–27.
Restrepo, J.D., Alvarado, E.M., 2011. Assessing major environmental issues in the Caribbean and Pacific coasts of Colombia, South America: an overview of fluvial fluxes, coral reef degradation, and mangrove ecosystems impacted by river diversion. In: Treatise on Estuarine and Coastal Science. Academic, Waltham, pp. 289–314.
Restrepo, J.D., Kjerfve, B., 2000. Water discharge and sediment load from the western slopes of the Colombian Andes with focus on Rio San Juan. J. Geol. 108, 17–33.
Rodriguez-Rubio, E., Stuardo, J., 2002. Variability of photosynthetic pigments in the Colombian Pacific Ocean and its relationship with the wind field using ADEOS-I data. J. Earth Syst. Sci. 111, 227–236.
Rommerskirchen, F., Plader, A., Eglinton, G., Chikaraishi, Y., Rullkötter, J., 2006. Chemotaxonomic significance of distribution and stable carbon isotopic composition of long-chain alkanes and alkan-1-ols in C4 grass waxes. Org. Geochem. 37, 1303–1332.
Rueda-Roa, D.T., Muller-Karger, F.E., 2013. The southern Caribbean upwelling system: sea surface temperature, wind forcing and chlorophyll concentration patterns. Deep Sea Res. I 78, 102–114.
Schlesinger, W.H., Melack, J.M., 1981. Transport of organic carbon in the world's rivers. Tellus 33, 172–187.
Schouten, S., Hopmans, E.C., Sinninghe Damsté, J.S., 2013. The organic geochemistry of glycerol dialkyl glycerol tetraether lipids: a review. Org. Geochem. 54, 19–61.
Sinninghe Damsté, J.S., Hopmans, E.C., Schouten, S., van Duin, A.C.T., Geenevasen, J.A.J., 2002. Crenarchaeol: the characteristic core glycerol dibiphytanyl glycerol tetraether membrane lipid of cosmopolitan pelagic crenarchaeota. JLR (J. Lipid Res.) 43, 1641–1651.
Sinninghe Damsté, J.S., Rijpstra, W.I.C., Hopmans, E.C., Weijers, J.W.H., Foesel, B.U., Overmann, J., Dedysh, S.N., 2011. 13, 16-Dimethyl octacosanedioic acid (iso-diabolic acid), a common membrane-spanning lipid of Acidobacteria subdivisions 1 and 3. Appl. Environ. Microbiol. 77, 4147–4154.
Sinninghe Damsté, J.S., Rijpstra, W.I.C., Hopmans, E.C., Foesel, B., Wü, P., Overmann, J., Tank, M., Bryant, D., Dunfield, P., Houghton, K., Stott, M., 2014. Ether- and ester-bound isodiabolic acid and other lipids in Acidobacteria of subdivision 4. Appl. Environ. Microbiol. 80, 5207–5218.
Sinninghe Damsté, J.S., 2016. Spatial heterogeneity of sources of branched tetraethers in shelf systems: the geochemistry of tetraethers in the Berau River delta (Kalimantan, Indonesia). Geochem. Cosmochim. Acta 186, 13–31.
Smith, R.W., Bianchi, T.S., Li, X., 2012. A re-evaluation of the use of branched GDGTs as terrestrial biomarkers: implications for the BIT Index. Geochem. Cosmochim. Acta 80, 14–29.
Simoneit, B.R., 1984. Organic matter of the troposphere—III. Characterization and sources of petroleum and pyrogenic residues in aerosols over the western United States. Atmos. Environ. 18, 51–67.
Toro, P.P.V., Bedoya, L.F.V., Correa, I.D., Franco, G.R.B., Alcántara-Carrió, J., Baena, J.A.P., 2016. Impact of terrestrial mining and intensive agriculture in pollution of estuarine surface sediments: spatial distribution of trace metals in the Gulf of Urabá, Colombia. Mar. Pollut. Bull. 111, 311–320.
Urakawa, H., Martens-Habbena, W., Huguet, C., de la Torre, J.R., Ingalls, A.E., Devol, A.H., Stahl, D.A., 2014. Ammonia availability shapes the seasonal distribution and activity of archaeal and bacterial ammonia oxidizers in the Puget Sound Estuary. Limnol. Oceanogr. 59 (4), 1321–1335.
Wang, Z., Fingas, M., Page, D.S., 1999. Oil spill identification. J. Chromatogr. A 843, 369–411.
Weijers, J.W.H., Schouten, S., van den Donker, J.C., Hopmans, E.C., Sinninghe Damsté, J.S., 2007. Environmental controls on bacterial tetraether membrane lipid distribution in soils. Geochem. Cosmochim. Acta 71, 703–713.
Whyte, F.S., Taylor, M.A., Stephenson, T.S., Campbell, J.D., 2008. Features of the Caribbean low level jet. Int. J. Climatol.: A J. R. Meteorol. Soc. 28, 119–128.
Zonneveld, K.A.F., Versteegh, G.J.M., Kasten, S., Eglinton, T.I., Emeis, K.C., Huguet, C., Mollenhauer, G., 2010. Selective preservation of organic matter in marine environments; processes and impact on the sedimentary record. Biogeosciences 7, 483–511.